Role of Structural Changes in the Triplet−Triplet Energy Transfer Process to Oxime Derivatives

Jacques Lalevée, Xavier Allonas,* Frédéric Louërat, and Jean Pierre Fouassier

Département de Photochimie Générale, 3 rue Alfred Werner, 68093 Mulhouse, France

Received: March 29, 2002; In Final Form: May 27, 2002

The triplet energy accepting properties of bridged hydroxy and methyl derivatives of acetophenone oxime were examined. Sandros and Agmon−Levine−Balzani (ALB) models were used to deduce the oxime triplet energies, E_T^O, and the reorganizational intrinsic barriers, $\Delta G^{\#}(0)$, associated with the reaction. It is found for the first time that these compounds exhibit different degrees of nonvertical energy transfer (NVET) behavior, depending on their chemical structure. These structural properties have been investigated at both the AM1 and the B3LYP/6-31+G(d) levels of theory. The flexibility of the ground-state molecule and the structural changes occurring during the $S_0 \rightarrow T_1$ sensitized transition seem to play crucial roles. It appears that two important rearrangements are involved, namely, rotation about the C−N double bond and a π system flattening associated with a torsion about the formal C−C single bond. To relate the NVET character to these structural changes, the energy variations associated with these latter were evaluated and successfully related to $\Delta G^{\#}(0)$. Moreover, the role of the thermal activation of the molecular coordinates is evidenced through the calculations of the ground and triplet potential energy surfaces (PESs) at DFT and CIS levels. A simple model, based on the Sandros equation, was derived to include the influence of such torsional modes on the energy-transfer behavior. Finally, the experimental quenching data were fitted to this model, leading to the conclusion that, although both C−N double bond and C−C single bond torsions occur during the sensitization, the thermal activation of C−C single bond torsion plays the major role in the NVET character of oxime derivatives.

Introduction

Molecular photosensitization through energy transfer represents an important process in the chemistry of life and thus has led to a great interest. Among the different ways for energy to transfer from one molecule to another, triplet−triplet energy transfer via an exchange mechanism between free diffusing species has received considerable attention.[1−12]

The excited energy level of the triplet state can be estimated by spectroscopic methods such as conventional absorption (heavy atom perturbation) or luminescence.[7,13−14] Unfortunately, such determinations failed for the oximes studied, which required a systematic use of sensitization experiments to investigate their triplet states. This process can be described by the following mechanism:[9−10]

SCHEME 1

$$^3D + A \underset{k_{-d}}{\overset{k_d}{\rightleftharpoons}} [^3D\cdots A] \underset{k_{-en}}{\overset{k_{en}}{\rightleftharpoons}} [D\cdots {}^3A] \xrightarrow{k_{-d}} D + {}^3A$$

where k_d, k_{-d}, k_{en}, and k_{-en} stand for the rate constants of formation and dissociation of the encounter complex and the rate constants of energy transfer and back energy transfer, respectively. Assuming that k_{-en} and k_{en} are higher than the other rate constants, the Sandros equation, which involves a Boltzmann distribution of the two triplets in the encounter complex, can be applied.[15] This simple theory, used routinely as a guide for classical behavior, leads to the following equation for the quenching rate constant, k_q:

$$k_q = \frac{k_d}{1 + \exp\left(\frac{+\Delta G}{RT}\right)} \quad (1)$$

where ΔG is the difference between the acceptor triplet energy, E_T^A, and the donor triplet energy, E_T^D. From this equation, it can be seen that a reduction of the donor triplet energy (less than 3 kcal/mol above the acceptor triplet state) causes a drastic decrease of the rate constant as a consequence of its exponential dependence on ΔG.

However, different systems depart from this description[2−12] with rate constants in the endothermic region, which decrease much less dramatically than expected from eq 1. This behavior, termed nonvertical energy transfer (NVET), was already observed on stilbene or biphenyl derivatives and was ascribed to the geometrical change of the molecule between the ground and the excited states. This has been the subject of many discussions over the last four decades.[2−8,11−12,16]

In a previous paper, the lowest triplet states of *O*-acyloximes have been studied by means of laser absorption spectroscopy.[17] Besides the fact that the acyl moiety has no influence on the triplet energy, quenching experiments have revealed a clear NVET behavior for some of the molecules. Indeed, the Sandros model for the triplet energy transfer applied only in the case of rigid chromophores (fluorenone-*O*-acyloxime) but does not fit the experimental results obtained with flexible molecules (acetophenone-*O*-acyloxime). Therefore, a first set of compounds was used to clarify the behavior of oximes toward energy-transfer reaction, showing that two molecular rearrangements, π system flattening and C−N bond twist in the triplet state, are particularly important to affect the NVET character of the oximes.[18]

* To whom correspondence should be addressed. E-mail: X.Allonas@uha.fr. Tel: (+33) 3 8933 6874. Fax: (+33) 3 8933 6895.

10.1021/jp025857s CCC: $22.00
Published on Web 06/20/2002

SCHEME 2

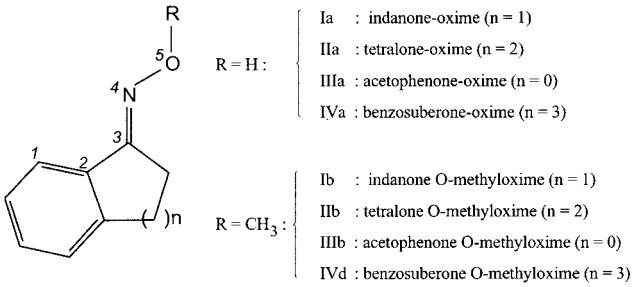

The aim of this paper is to control, by cyclization, the dihedral angle between the CN double bond and the phenyl ring of acetophenone−oxime derivatives and to explore the behavior of such compounds through energy-transfer experiments. The influence of the distortion of the π system in the ground-state molecule can thus be clearly examined. Successful attempts were made to relate experimental data to the results obtained by molecular modeling. Therefore, a simple model for NVET that takes into account the geometry changes involved in the energy-transfer reaction with oxime derivatives will be proposed.

Experimental Section

Synthesis of the Oximes. All oximes used in this study were synthesized from their parent ketones according to a procedure similar to that found in the literature[19] and are shown in Scheme 2. A total of 5 mmol of the starting ketone and 6 mmol of sodium hydroxide were mixed in 1 mL of ethanol and 2.5 mL of water. Hydroxyoximes were prepared by adding 3 mmol of hydroxylamine sulfate, and methyl-*O*-oximes were prepared by adding 6 mmol of methoxylamine hydrochloride. The mixture was stirred and refluxed for 2 h, extracted with ether, and dried with magnesium sulfate. The ether was removed under vacuum, and the oximes were crystallized from toluene and then sublimated before used.

The isomeric form of the oximes was characterized by ^{13}C NMR spectroscopy. Only one form was observed corresponding to the E isomer.[20−22] 1-Indanone oxime (**Ia**): white crystal; $\lambda_{max} = 252$ nm; ^1H RMN ($CDCl_3$) δ (ppm) 3.02 (m, 4H), 7.3 (m, 3H), 7.7 (d, 1H), 9.42 (s, 1H). 1-Tetralone oxime (**IIa**): white crystal; $\lambda_{max} = 251$ nm; ^1H RMN ($CDCl_3$) δ (ppm) 1.95 (m, 2H), 2.80 (t, 2H), 2.92 (t, 2H), 7.27 (m, 3H), 7.97 (d, 1H), 10.30 (s, 1H). 1-Acetophenone oxime (**IIIa**): white crystal; $\lambda_{max} = 245$ nm; ^1H RMN ($CDCl_3$) δ (ppm) 2.35 (s, 3H), 7.42 (m, 3H), 7.65 (m, 2H), 10 (s, 1H). 1-Benzosuberone oxime (**IVa**): white crystal; $\lambda_{max} = 236$ nm; ^1H RMN ($CDCl_3$) δ (ppm) 1.65 (t, 2H), 1.81 (t, 2H), 2.74 (m, 4H), 7.14 (d, 1H), 7.29 (m, 2H), 7.42 (d, 1H). 1-Indanone *O*-methyl oxime (**Ib**): colorless liquid; $\lambda_{max} = 257$ nm; ^1H RMN ($CDCl_3$) δ (ppm) 2.87 (t, 2H), 3.01 (t, 2H), 3.99 (s, 3H), 7.30 (m, 3H), 7.70 (d, 1H). 1-Tetralone *O*-methyl oxime (**IIb**): colorless liquid; $\lambda_{max} = 262$ nm; ^1H RMN ($CDCl_3$) δ (ppm) 1.84 (q, 2H), 2.72 (t, 4H), 3.99 (s, 3H), 7.21 (m, 3H), 7.98 (d, 1H). 1-Acetophenone *O*-methyl oxime (**IIIb**): colorless liquid; $\lambda_{max} = 250$ nm; ^1H RMN ($CDCl_3$) δ (ppm) 2.33 (s, 3H), 4.0 (s, 3H), 7.37 (m, 3H), 7.63 (m, 2H). 1-Benzosuberone *O*-methyl oxime (**IVb**): colorless liquid; $\lambda_{max} = 241$ nm; ^1H RMN ($CDCl_3$) δ (ppm) 1.61 (q, 2H), 1.76 (q, 2H), 2.65 (t, 2H), 2.74 (t, 2H), 3.98 (s, 3H), 7.12 (d, 1H), 7.25 (m, 2H), 7.40 (d, 1H).

Laser Setup. The nanosecond transient absorption setup is based on a pulsed Nd:YAG laser (Powerlite 9010, Continuum) operating at 10 Hz that delivers nanosecond pulses at 355 nm with an energy about 500 mJ. The laser pumps an optical parametric oscillator (Sunlite, Continuum) that generates narrow-band radiation in the visible and the near-infrared spectral region. After frequency doubling (FX1, Continuum), the wavelength is tunable from 225 to 1800 nm with an energy about 50 mJ at 550 nm. The transient absorption analysis system (LP900, Edinburgh Instruments) uses a 450 W pulsed xenon arc lamp, a Czerny-Turner monochromator, a fast photomultiplier, and a transient digitizer (TDS 340, Tektronix). This experimental setup is characterized by an instrumental response equal to 7 ns. All of the experiments were made in argon-saturated benzene solution (spectroscopic grade, Fluka), except for the ground-state absorption spectra that were made in acetonitrile (spectroscopic grade, Fluka).

Computational Procedure. All quantum calculations were carried out using MOPAC 6.0[23] for semiempirical methods or Gaussian 94W suite of programs[24] for ab initio calculations. Relaxed ground- and lowest triplet-state structures were first optimized using AM1 method. The resulting geometry for each of these electronic states was optimized at the HF level employing the 6-31G basis set. Further optimization was finally achieved using the B3LYP functional with the diffuse and polarized augmented basis set 6-31+G(d). All of the optimized geometries were frequency checked. Potential energy surfaces were computed using the B3LYP/6-31+G(d) method with a complete optimization of all geometrical parameters except the constrained dihedral angles α (C2C3NO) or β (C1C2C3N). Spectroscopic triplet energies corresponding to these structures are computed at both DFT and CIS levels. Zero-point energy (ZPE) terms were calculated from frequency calculations carried out at RHF or UHF/6-31+G(d) levels of theory.

Results and Discussion

Triplet Energy Transfer Experiments. A glance at the literature shows that planar $\pi\pi^*$ triplet states or $n\pi^*$ triplet states undergo vertical transition. In this work, the triplet donors were selected to meet this condition; as a consequence, nonvertical character can only result from the acceptor properties. The results concerning the quenching experiments of triplet donors with well-defined energy levels are collected in Table 1.

Despite the well-known example of *cis*- and *trans*-stilbene,[1−3,5] the treatments of NVET remain rather scarce in the literature. Therefore, the explanation of this phenomenon remains an exciting topic. The low slope of the quenching curves has led some authors to introduce an empirical parameter in the Sandros equation, but without supporting any theoretical background.[25] Furthermore, the idea that electron transfer (ET) and energy transfer (TT) are two conceptually related processes governed by the same theory of radiationless transition has led other groups to use different models based on Marcus ET theory.[26,27] Although this latter model was proved to account very well for the experimental data of *trans*- and *cis*-stilbene,[9] as well as for azobenzene,[27] the large number of spectroscopic parameters required and the assumptions that have to be made on the relative contribution of the relevant coordinates prevent any extensive use on most different systems. Therefore, in our case, the quenching rate constants were fitted with the classical Agmon−Levine−Balzani (ALB) model, which is known to give reliable results.[9,28−30] Within this framework and assuming the mechanism described in Scheme 1, the quenching rate constant, k_q, can be written as

TABLE 1: Triplet Energies, E_T^D, of the Donors Used and Quenching Rate Constants, k_q, Obtained in Benzene for the Quenching of Various Donors by the Oximes Studied

		log (k_q)							
	E_T^D (kJ/mol)	**Ia**	**Ib**	**IIa**	**IIb**	**IIIa**	**IIIb**	**IVa**	**IVb**
xanthone	310	9.8	9.86	9.8	9.87	9.75	9.8	9.8	9.57
4,4′-dimethoxybenzophenone	292		9.6	9.64	9.58		9.4	9	8.99
benzophenone	287	9.52	9.45	9.46	9.45	9.4	9.34	8.75	8.62
phenanthrene	260	9.18	9.37	9.1	9.33	8.73	8.97	7.57	7.73
4-phenylbenzophenone	255	9.1	9.11	9	9.13	8.57	8.76	7.5	7.76
9-cyanophenanthrene	243	8.16	8.63	8.4	8.95	7.81	8.36	6.6	7.13
chrysene	238	7.38	7.72	7.76	8.27	7.16	7.62	6	6.58

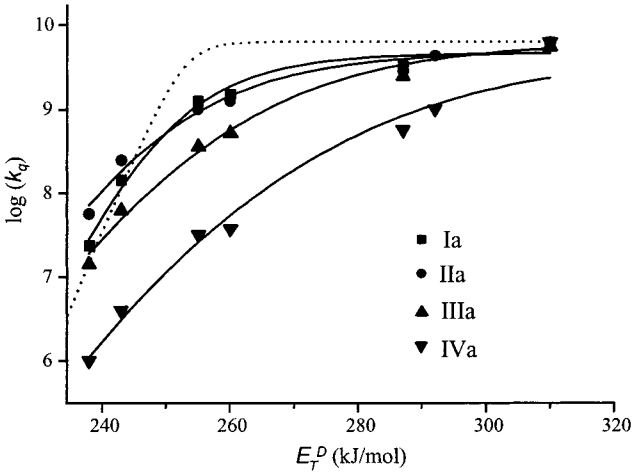

Figure 1. Plots of the quenching rate constants vs the donor triplet energy and corresponding best fits obtained applying the ALB model for hydroxyoximes. A Sandros best fit is also reported in dotted line for **Ia**.

$$k_q = \frac{k_d}{1 + \frac{k_{-d}}{k_{en}} + \exp\left(\frac{+\Delta G}{RT}\right)} \quad (2)$$

where k_{en} is expressed according to the classical model of the absolute rate theory by

$$k_{en} = k_{en}^0 \exp\left(\frac{-\Delta G^{\#}}{RT}\right) \quad (3)$$

k_{en}^0 and $\Delta G^{\#}$ are the preexponential factor and the standard free activation energy, respectively. The key point in this treatment is the relationship between $\Delta G^{\#}$ and ΔG, which is given by

$$\Delta G^{\#} = \Delta G + \frac{\Delta G^{\#}(0)}{\ln 2} \ln\left(1 + \exp\left(-\frac{\Delta G \ln 2}{\Delta G^{\#}(0)}\right)\right) \quad (4)$$

where $\Delta G^{\#}(0)$ is the reorganizational intrinsic barrier related to the changes in nuclear positions that have to occur prior the energy transfer.

Both Sandros and ALB models were used to fit the experimental data. Figure 1 shows the different fits obtained for the hydroxyoximes, and the entire results are gathered in Table 2. In the case of the indanone oxime derivatives **Ia** and **Ib**, the fits obtained with the Sandros model agree satisfactorily with the experimental results. The triplet energies, E_T^O, obtained from Sandros and ALB models are also very close for these two compounds. These facts clearly support a vertical behavior for these derivatives.

For the other compounds, the Sandros model poorly described the experimental data, contrary to the ALB treatment. Indeed,

TABLE 2: Results Obtained from the Sandros and ALB Models for the Energy-Transfer Reaction with the Oximes Studied

	Sandros	ALB		
oxime	E_T^O (kJ/mol)	E_T^O (kJ/mol)	k_{en}^0 ($\times 10^{-10}$ s^{-1})	$\Delta G^{\#}(0)$ (kJ/mol)
Ia	252 ± 1.5	248 ± 1.9	0.83 ± 0.4	7.8 ± 2
IIa	251 ± 1.8	238 ± 5.9	0.95 ± 0.5	12 ± 3.5
IIIa	256 ± 2.4	240 ± 5	1.16 ± 0.7	15 ± 3.5
IVa	265 ± 2.7	242 ± 6	1[a]	21 ± 2
Ib	250 ± 1.5	244 ± 2.9	0.77 ±0.4	7.3 ± 3
IIb	248 ± 1.6	229 ± 17	0.97 ±0.7	13 ± 7.5
IIIb	252 ± 2.3	232 ± 13	0.8 ±0.7	15 ± 6.5
IVb	261 ± 3.2	220 ± 10	1[a]	27 ± 3.5

[a] Values fixed to reach a convergence.

TABLE 3: Molecular Coordinates of the Different Oximes Used in the Relaxed Ground and Triplet States Obtained with the (U)B3LYP/6-31+G(d) Method

	dihedral angle		bond length		spin density		relaxed triplet energy
compound (electronic state)	α (deg)	β (deg)	C−C (Å)	C=N (Å)	C	N	(kJ/mol)
Ia (S_0)	180	0.0	1.468	1.283			
Ia (T_1)	96.4	5.9	1.420	1.389	0.70	0.81	213
IIa (S_0)	179.4	11.0	1.484	1.289			
IIa (T_1)	95.7	0.6	1.426	1.401	0.72	0.82	203
IIIa (S_0)	179.6	20.4	1.488	1.288			
IIIa (T_1)	93.8	2.8	1.430	1.403	0.77	0.825	205
IVa (S_0)	177.8	42.8	1.491	1.288			
IVa (T_1)	−98.4	11.5	1.437	1.407	0.80	0.82	211

the E_T^O values obtained for these molecules from the ALB model are always lower than the Sandros results. An interesting feature is that similar E_T^O values were obtained for all of the compounds studied, the variation being about 10 kJ for hydroxyloximes and 20 kJ for methyloximes. Despite the strongly different quenching curves, these closely related molecules are expected to have similar triplet energy levels (Table 3). In a former paper,[17] it was observed that for different *O*-acyl-substituted oximes, the acyl moiety has only a slight effect on the triplet energy and the orbitals involved in the S_0-T_1 transition were localized on the oxime moiety. In the present case, replacing the hydrogen atom by a methyl group slightly decreases the triplet energy level, but no significant change of the slope in the endergonic region was observed. Therefore, the ALB model appears to describe fairly well the quenching plots, with deduced E_T^O values that are consistent with the structure of the compounds. The difference between both models can be ascribed to an increase of the NVET character from **IIa,b** to **IVa,b**, which is not accounted for by the Sandros model. Because very close E_T^O values were found for the different oximes studied, the NVET character cannot be ascribed to energy level changes and will be related to geometric changes. It could be seen from Figure 1 and Table 2, at least qualitatively, that the nonvertical character is related to the $\Delta G^{\#}(0)$ parameter.

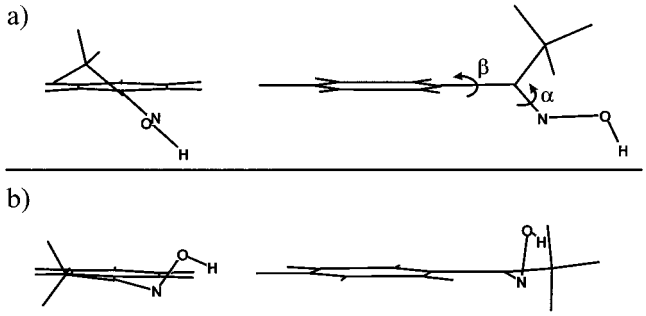

Figure 2. Molecular geometry of acetophenone oxime **IIIa** in (a) the ground state and (b) the relaxed triplet state.

The values were found to strongly vary from 7.3 kJ/mol for **Ib** to 27.0 kJ/mol for **IVb** as a consequence of the decrease of the slope in the endergonic region. Therefore, in the following, $\Delta G^{\#}(0)$ will be used as an empirical measurement of the NVET character.

Ground- and Triplet-States Equilibrium Structures. Despite the qualitatively good equilibrium structures obtained with the AM1 Hamiltonian, it is more convenient to focus the discussion on the B3LYP/6-31+G* results obtained only with hydroxyoximes (**Ia** to **IVa**), the difference between *O*-methyl-substituted oximes and hydroxyoximes being not significant. It was found that for hydroxyoximes (Table 3) the dihedral angle α (C2C3NO) is about 180° in the ground state whereas the dihedral angle β (C1C2C3N) varies from 0° (**Ia**) to 42.8° (**IVa**). As expected, this effect is ascribed to the different bridges introduced in the basic structure of acetophenone oxime, **IIIa**. Indeed, the five-membered ring of **Ia** gives a planar geometry at the ground state, in contrast to the six- or seven-membered ring systems of **IIa** and **IVa**, respectively, which distorted the planarity of the π system. As observed in a previous work,[18] the flexible structure of **IIIa** exhibits an intermediate twisted geometry, β being 20.4°.

As it can be seen in Figure 2, the situation is by far different in the triplet state. Considering that an electron is promoted from the C−N π bonding orbital to the corresponding π^* antibonding orbital, torsion of this bond should occur to avoid singly occupied orbital interaction. Therefore, α varies from about 180° to around 95° (Table 3), with a spin density mainly distributed on the C3 and N atoms (about 0.7−0.8 on each atom). This gives a manifest biradical character to the triplet state, as already mentioned in the literature.[31] This situation is very similar to that observed for olefin triplet states.[13,32] In addition, β was found to decrease in the triplet state, ranging from 0.6° (**IIa**) to 11.5° (**IVa**), leading to a more planar structure of the carbon skeleton. This fact can be accounted for by a stabilization due to the delocalization of the lone electron of the carbon atom with a flattening of carbon skeleton. This effect is reflected in this spin density, which decreases with β in the triplet state. Moreover, an important decrease of the C2−C3 bond length underlines this delocalization, giving to this bond a partial double-bond character (Table 3).

The relaxed triplet energies were computed as the energy difference between the relaxed triplet and ground states. DFT methods have been shown to give reliable values in the case of polyolefin triplet-state calculations.[29,32] In the present case, the values obtained (Table 3) are slightly lower than the experimental ones (from ∼34 kJ/mol), a fact already noticed for polyenes.[32]

From these results, it appears that two main structural changes occur between the relaxed ground and triplet states: a decrease of β, which leads to a more planar carbon skeleton, and a twist along the C3N bond. The consequence of such structural changes on the NVET character will be now discussed in detail.

TABLE 4: Calculated Energy Values for the Torsion in the Ground State, $E_{tor}(\alpha)$ along α and $E_{tor}(\beta)$ along β, to Reach the Corresponding Triplet-State Geometry

	AM1		B3LYP/6-31+G(d)	
molecule	$E_{tor}(\alpha)$ (kJ/mol)	$E_{tor}(\beta)$ (kJ/mol)	$E_{tor}(\alpha)$ (kJ/mol)	$E_{tor}(\beta)$ (kJ/mol)
Ia	95.5	0.33	229.4	0.2 (0.24[a])
Ib	95.1	0.33		
IIa	90.6	0.88	236.2	0.5 (0.6[a])
IIb	89.8	0.84		
IIIa	102.0	3.14	229.9	0.2 (0.6[a])
IIIb	101.8	3.33		
IVa	103.2	7.7	261.2	11.3 (12.2[a])
IVb	102.4	9.1		

[a] ZPE-corrected values.

Thermal Bond Activation Mechanism. The NVET phenomenon is generally observed for flexible molecules that have different relaxed ground- and triplet-state conformations. To explain such an effect, it was suggested that molecules can explore different configurations within the encounter complex to reduce the energetic requirement of the process.[1,6,8,16] However, some authors have argued that NVET involves no greater geometric distortions than those corresponding to spectroscopic transitions.[14] These two points of view can be unified assuming vertical transitions from different conformations of the acceptor molecule that are accessible by thermal activation; such a hot-band mechanism has already been invoked to explain the NVET behavior of stilbene derivatives.[1,2,6,11,16] Some thermally activated structures can be reached for which the transition energy to the triplet state is lower than the spectroscopic one. Depending on the energy available from the donor, only a part of the thermally activated molecules can be promoted to their triplet state. Therefore, the quenching rate constant is expected to decrease much more slowly when geometric changes are involved for the transition, leading to a clear NVET behavior. From this point of view, the NVET character is strongly connected to the relevant geometry changes.[1,8,11,18] For stilbene derivatives, it has been supposed that the double-bond torsion plays the major role in this activation. In the present study, a detailed investigation of the influence of the structural changes occurring during the sensitized transition is expected to bring out some useful information about the specific behavior of oxime derivatives toward triplet energy transfer.

A first approach to examine the NVET assumes that, if the thermal activation of some coordinates can be operative, the character of the NVET should be connected with the energy associated with the relevant change in geometry, that is, $\Delta G^{\#}(0)$ should be related to the energy of torsion, E_{tor}, required to twist the considered dihedral angle from its ground-state to its triplet-state value.[18] It is therefore reasonable to assume that a large change of E_{tor} can cause a large variation in the NVET behavior.

On the basis of the two important conformational changes previously underlined between the ground and the triplet states, the energy differences, E_{tor}, were computed for both α and β dihedral angles (respectively, $E_{tor}(\alpha)$ and $E_{tor}(\beta)$) and for different compounds using the HF/AM1 method for all of the oximes studied and the B3LYP/6-31+G* level for the hydroxyoximes. The results are gathered in Table 4. The $E_{tor}(\alpha)$ values are very similar for all of the compounds studied, spanning from 90 to 100 kJ/mol at the AM1 level and from 230 to 260 kJ/mol at the B3LYP level. The difference between the results obtained

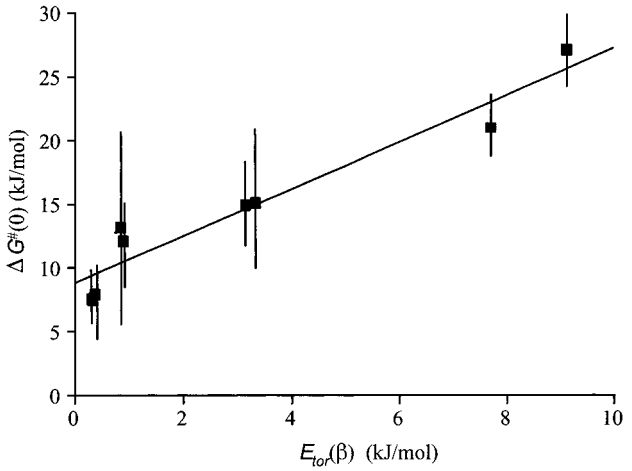

Figure 3. Plot of the torsion energy, E_{tor}, associated with the variation of β in the ground state as a function of the reorganizational intrinsic energy, $\Delta G^{\#}(0)$.

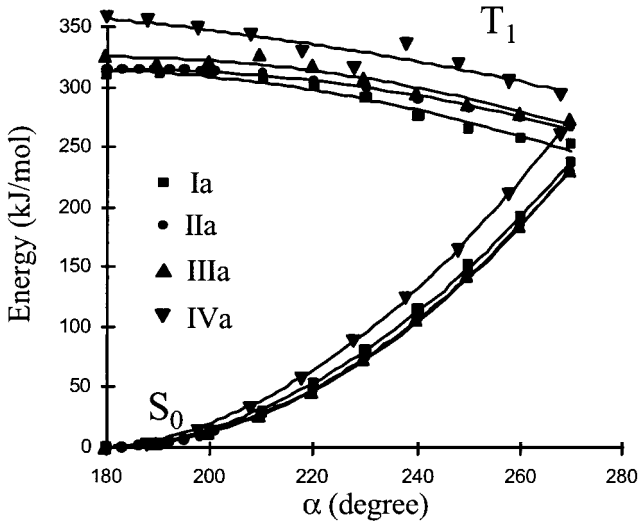

Figure 4. Potential energy surfaces for hydroxyoximes along the double-bond coordinate, α.

with the calculations is ascribed to the poorest description of the electronic repulsion of the twisted geometry $\alpha = 270°$ at the AM1 level. However, both methods show qualitatively that the $E_{tor}(\alpha)$ values are very similar, in contrast to the $\Delta G^{\#}(0)$ values, which vary strongly. This clearly demonstrates the lack of correlation between $E_{tor}(\alpha)$ and $\Delta G^{\#}(0)$.

In contrast, $E_{tor}(\beta)$ values associated with a torsion along β increase with increasing $\Delta G^{\#}(0)$, spanning from 0.33 to 9.1 kJ/mol at the AM1 level, as shown in Figure 3. This clear correlation between $E_{tor}(\beta)$ and $\Delta G^{\#}(0)$ indicates that the torsion along the C1C2C3N single bond, and therefore the distortion of the π system, plays an important role in the NVET behavior of oxime derivatives, albeit this correlation results from a crude approach. The values obtained for hydroxyoximes using the DFT method led to the same conclusion.

It appears that the NVET character depends on the single-bond torsion mode and not on the double-bond one. A similar conclusion has been deduced for styrene derivatives from purely experimental work.[33] However, this approach, although it has been shown to be qualitatively very useful,[18] remains rather crude and does not give any quantitative information about the role of the thermal bond activation in this process. Moreover, it must be noticed that only thermally activated structures favored from the Boltzmann distribution law participate significantly in the sensitization reaction. From this point of view, low values of $E_{tor}(\beta)$ compared to $E_{tor}(\alpha)$ favor this thermal activation, a fact that is in line with the clear correlation between $E_{tor}(\beta)$ and $\Delta G^{\#}(0)$.

Potential Energy Surface Associated with the Torsion Coordinates. To test the validity of the thermal bond activation mechanism involving an acceptor that is thermally activated along the relevant coordinates, the potential energy surfaces (PESs) corresponding to the above-mentioned bond torsions were calculated for both ground and triplet states at the (U)B3LYP/6-31+G(d) level. These PESs were calculated by constraining the relevant coordinates at different values and calculating the corresponding ground and spectroscopic triplet energies. Therefore, these energies quoted in Figures 4 and 5 are relative values with respect to the relaxed ground state of each molecule. Calculations with the CIS method were also performed to get more insight in the variation of this spectroscopic parameter with α or β.

Figure 4 shows the PESs along the double-bond torsion for hydroxyoximes **Ia** to **IVa**. A 90° torsion of the double bond from 180° to 270° requires, in the ground state, about 230−260 kJ/mol. From the spectroscopic triplet state, the same torsion leads to a stabilization of 47, 59, 53, and 61 kJ/mol for **Ia**, **IIa**, **IIIa**, and **IVa**, respectively, at the DFT level. From Figure 4, it can be observed that thermal activation at room temperature (assuming 5 kJ/mol of thermal activation) does not lead to a large exploration of the ground-state curve. Indeed, one can expect a variation of about $\alpha_{eq} \pm 10°$ around the equilibrium geometry. The decrease in the triplet-state curve associated with this variation of α is less than 1.0 kJ/mol (except **IIIa** for which the decrease is about 5 kJ/mol), a value that is negligible. For sake of clarity, spectroscopic triplet energies at the CIS level are not given in Figure 4, a similar effect being observed with a decrease lower than 5 kJ/mol for all of the compounds studied. Therefore, the overall decrease in the transition energy due to thermal activation only originates from the thermal energy gained in the ground state. Although this effect can be operative to some extent, this energy is too small to account alone for the large variation in the NVET character exhibited by the different oximes studied. Moreover, it should be noticed from Figure 4 that the PESs obtained for the different structures are very similar, although the NVET character is strongly dependent on the structure. This conclusion falls into line with the lack of correlation between $\Delta G^{\#}(0)$ and $E_{tor}(\alpha)$.

The situation is by far different in the case of a single-bond torsion associated with the β dihedral angle. Indeed, from Figure 5, it can be seen that the corresponding PESs along the dihedral angle β for the hydroxyoximes are very different from one molecule to another. For triplet energies, both DFT and CIS results are given. The latter method systematically gives spectroscopic triplet energies about 50 kJ/mol lower than the DFT method. However, a very similar evolution of the triplet energies can be observed giving confidence to the results obtained in the variation of E_T with β (Figure 5).

In the case of **Ia**, the PES of the ground state can be fitted with a parabola, reflecting the in-plane symmetry of the molecule. The lowest triplet-state PES is nearly located at the same molecular coordinate as the relaxed ground state. For the corresponding spectroscopic states, the observed PES is also parabolic. For a thermal activation of 5 kJ/mol along the ground-state curve, a maximum variation of only 3 kJ/mol (computed at DFT level and 2.5 kJ/mol at CIS level) of the energy required for the transition can be observed strongly supporting the vertical behavior of **Ia** and **Ib**.

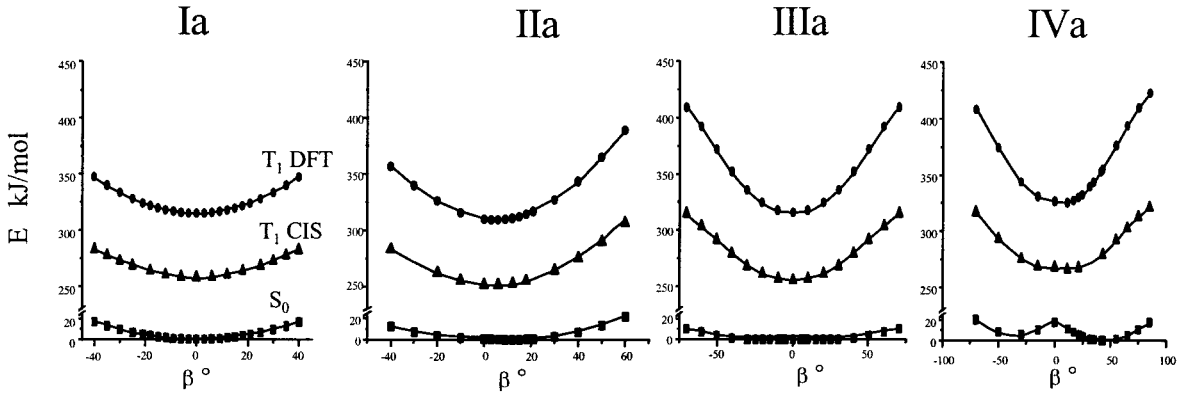

Figure 5. Potential energy surfaces for hydroxyoximes (**Ia** to **IVa**) along the single-bond coordinate, β: (■) S_0 level; (▲) T_1 CIS level; (●) T_1 DFT level.

The PES profile of the triplet state of **IIa** is qualitatively similar to that of **Ia**. However, the ground-state PES is asymmetric and flatter. In a similar manner, a thermal activation of 5 kJ/mol of the ground-state molecule leads to a variation of 13 kJ/mol (computed at the DFT level and 10 kJ/mol at the CIS level) of the energetic requirement for the transition. Contrary to **Ia**, triplet energy transfer can occur from different ground-state conformations associated with different spectroscopic triplet energies, resulting in a slight but significant nonvertical character.

This situation is more pronounced in the case of **IIIa**. The equilibrium structures for the ground state and the triplet state are, respectively, $\beta = 20.4°$ and 2.8°. Indeed, the ground-state PES flattens out with a double-well-like shape due to a nearly freely rotating phenyl ring along the considered single bond. Therefore, thermal activation can populate a large number of different ground-state geometries, affecting the required excitation energy to reach the triplet state. A thermal activation of 5 kJ/mol can strongly affect the spectroscopic triplet energy of this compound with values of 290 and 255 kJ/mol corresponding to β angles of 0° and 55°, respectively, at CIS level. DFT results predict a variation of 52 kJ/mol associated with a similar modification of this dihedral angle. This important result demonstrates how thermal activation of this bond torsion is of great benefit for affecting the energy required for the transition.

This is exemplified in the case of **IVa**. For this compound, the ground-state PES presents a clear double-well behavior, the conformation of higher energy being 5.8 kJ/mol more energetic than the stable conformation, with an 18 kJ/mol barrier. The dihedral angle β for the more stable structure is located at 42.8°. However, an important distribution of molecules can be assumed because of the low energy requirement associated with a β variation. Moreover, the vertical energy is strongly related to this angle. For example, a thermal activation of about 5 kJ/mol around the more stable ground-state structure is related to a variation of the spectroscopic energy of about 62 and 36 kJ/mol at DFT and CIS levels, respectively.

As can be seen from these examples, a slight variation in energy along β of the ground-state molecule can greatly affect the energetic requirement of the reaction allowing low-energy donors to transfer the excitation energy to a part of the acceptor molecules that are thermally activated enough. This character is therefore directly influenced by the shape and the respective positions of the S_0 and T_1 PESs. Contrary to previous works on stilbene derivatives, from the calculations performed along α and β dihedral angles, it appears for oximes that the β torsion should play the major role in the NVET behavior.

Rationalization of the Thermal Bond Activation Mechanism. Although it is now clear that the thermal bond activation can change the transition energy, one should say that the ALB model used in the first part of this paper to deduce E_T^O is not capable of dealing explicitly with this effect. In the following, a simple model derived from the Sandros treatment is introduced. Indeed, for a vertical transition involving mainly one ground-state conformation (**Ia**, **Ib**), this treatment seems particularly adequate.[15,18,25] Therefore, an attempt was made to introduce into this model the specific effect of the conformational distribution of the thermal population along a molecular coordinate.

To rationalize such an approach, the PESs are assumed to be described by parabolic curves. For the compounds studied, this assumption is valid in the case of a small activation through thermal energy. Therefore, at each angle θ along the considered torsion mode, the energy $E_T(\theta)$ required to reach the triplet curve is given by

$$E_T(\theta) = E_{T_{min}} + \frac{1}{2}b_T(\theta - \theta_{T_{min}})^2 - \frac{1}{2}b_G(\theta - \theta_{G_{min}})^2 \quad (5)$$

where $E_{T_{min}}$ corresponds to the difference between the minimum of the triplet-state PES and that of the ground-state one. $\theta_{T_{min}}$ and $\theta_{G_{min}}$ are the values of the angles for the lowest energies of the triplet- and the ground-state PESs, respectively, and b_T and b_G are the corresponding coefficients of the parabolic PESs. Working with $\Delta\theta = \theta_{G_{min}} - \theta_{T_{min}}$ leads to the following expression:

$$E_T(\theta) = E_{T_{min}} + \frac{1}{2}b_T\theta^2 - \frac{1}{2}b_G(\theta - \Delta\theta)^2 \quad (6)$$

Therefore, using the simple Sandros expression for the rate constant of quenching, $k_q(\theta)$, at a given angle gives

$$k_q(\theta) = \frac{k_d}{1 + \exp\left(\frac{E_T(\theta) - E_T^D}{RT}\right)} \quad (7)$$

The normalized population, $w(\theta)$, for each geometry is given by the Boltzmann law:

$$w(\theta) = \frac{\exp\left(-\frac{\frac{1}{2}b_G(\theta - \theta_{G_{min}})^2}{RT}\right)}{\sum_\theta \exp\left(-\frac{\frac{1}{2}b_G(\theta - \theta_{G_{min}})^2}{RT}\right)} \quad (8)$$

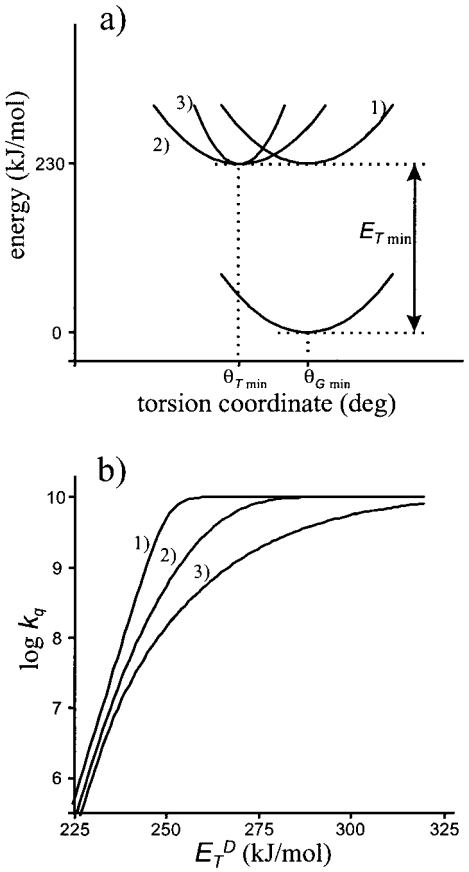

Figure 6. Examples of (a) triplet PESs exhibiting the same ground-state equilibrium geometry and (b) corresponding quenching plots according to the thermal bond activation model.

Taking into account the thermal population of each geometry into the expression of the overall quenching rate constant, k_q, leads to

$$k_q = \sum_{\theta} w(\theta) k_q(\theta) \tag{9}$$

Figure 6 shows some curves simulated by using eqs 5−9 with different profiles for the triplet PES. It can be seen that both the topology and the position of PESs strongly affect the quenching plot. Similar curves for triplet and ground states centered at the same coordinate (curve 1, $E_{T_{min}} = 250$ kJ/mol, $\Delta\theta = 0°$, $b_T = b_G = 2 \times 10^{-2}$ kJ/deg^2) lead to a vertical behavior. Thermal activation allows one to explore the ground-state surfaces but does not lead to any geometry from which the triplet state can be reached with a different energy. When the equilibrium position of the triplet PES shifts along the molecular coordinate (curve 2, $E_{T_{min}} = 250$ kJ/mol, $\Delta\theta = 40°$, $b_T = b_G = 2 \times 10^{-2}$ kJ/deg^2), the quenching plot flattens out because all of the ground-state molecules do not have the same probability of reaction depending on their conformation. Such a situation is more pronounced when the coefficient b_T of the triplet state increases or b_G decreases (curve 3, $E_{T_{min}} = 250$ kJ/mol, $\Delta\theta = 0°$, $b_T = 3b_G = 6 \times 10^{-2}$ kJ/deg^2). In this case, because of a low b_G value, an important distribution of molecules along β is expected. Moreover, because of high b_T and $\Delta\theta$ values, important changes of the energetic requirement for the process can be supposed. Such a situation leads to a large distribution of $E_T(\theta)$ values and therefore to a NVET behavior characterized by a flattening out of the quenching plots.

The experimental k_q data obtained for the hydroxyoximes were fitted with this model. Figure 7 shows the relevant

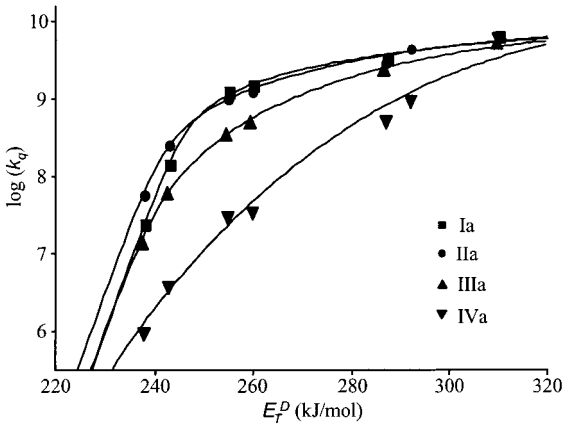

Figure 7. Experimental data fitted by the model based on the thermal bond activation mechanism.

TABLE 5: Calculated Values of the Parabolic Coefficients Corresponding to the Torsions along the Dihedral Angles α (C2C3NO) and β (C1C2C3N)[a]

	double bond C2C3NO	single bond C1C2C3N	fitting parameters		
oxime	b_G; b_T ($\times 10^2$ kJ/deg^2)	b_G; b_T ($\times 10^2$ kJ/deg^2)	b_G; b_T ($\times 10^2$ kJ/deg^2)	$\Delta\theta$ (deg)	E_T^O (kJ/mol)
Ia	5.8; −1.2	2.1; 4.1	5.6; 7.8	36	260
IIa	6.1; −1.8	1.3; 3.8	8.0; 6.9	39	247
IIIa	5.8; −1.3	0.3; 4.4	0.99; 5.6	45	250
IVa	6.4; −2.1	2.0; 5.8	1.5; 3.0	70	246

[a] Parameters deduced from the best fits with eqs 5−9.

quenching data together with the best fits obtained from eqs 5−9, and the results were collected in Table 5. In can be seen that the model fits fairly well all of the data for each oxime and perfectly accounts for the NVET character of the compounds. In particular, data corresponding to **IIIa** exhibit a change in the curvature of the endergonic region that is well-reproduced by the model.

It is interesting to note that very similar triplet energy levels are obtained for the compounds studied despite the very different quenching curves observed. These values are very consistent with those obtained from the ALB model, being about 4−12 kJ/mol higher than these latter. From a qualitative point of view, the fitting results can be compared to those obtained by molecular calculations. The $\Delta\theta$ parameter increases from 36° to 70° from **Ia** to **IVa**; a similar trend is observed in the results of molecular modeling with a $\Delta\theta$ value increasing from about 0° to 43° in the same series. The determined values of b_T and b_G can be compared to that obtained from the parabolic fit of the PES calculated at the DFT level. From Table 5, it can be seen that the agreement is better with values calculated from the single-bond torsion than those for the double-bond one, demonstrating the importance of such mode in NVET character of oximes. For the compounds **IIIa** and **IVa**, a relatively good agreement between calculated and fitting parameters can be observed. Despite the relatively correct values of b_T and b_G, for **Ia** and **IIa**, the $\Delta\theta$ values obtained by the fitting procedure are found to be higher than those obtained from calculations. Deviation between these values can be due to the slight influence of other geometrical distortions (C−C or C=N bond length changes), which are actually neglected in the calculation of b_G and b_T. From a general point of view, the good agreement assesses that this model, albeit rather simple, allows a proper description of the effect of thermal bond activation on the NVET character of the oximes studied.

Conclusion

This paper outlines for the first time the NVET character of different oxime derivatives in triplet−triplet sensitization experiments. The degree of NVET was probed through the value of $\Delta G^{\#}(0)$ obtained by applying the ALB model. Calculations on ground and triplet states reveal that double-bond torsion is inefficient to explain the NVET behavior. On the contrary, it was shown that thermal activation of single bond can lead to a drastic modification of the spectroscopic triplet energy of the acceptor and to a large NVET character for a flexible oxime. These results can be compared to those obtained on stilbene derivatives for which the double-bond torsion is supposed to play the major role. This contrasting behavior underlines the importance of extending this work on other chromophores to get more insight into the structural influences on the triplet−triplet sensitization reaction.

Acknowledgment. Thanks are due to Dr Chantal Daniel (CNRS Strasbourg, France) for helpful discussions on computational methods.

References and Notes

(1) Lamola, A. A. Electronic energy transfer in solution: Theory and applications. In *Techniques of Organic Chemistry*; Weisberger, A., Ed.; Wiley: New York, 1969; Vol. 14.

(2) Saltiel, J.; Charlton, J. L.; Mueller, W. B. *J. Am. Chem. Soc.* **1979**, *101*, 1347.

(3) Hammond, G. S.; Saltiel, J. *J. Am. Chem. Soc.* **1963**, *85*, 2516.

(4) Herkstroeter, W. G.; Hammond, G. S. *J. Am. Chem. Soc.* **1966**, *88*, 4769.

(5) Hammond, G. S.; Saltiel, J.; Lamola, A. A.; Turro, N. J.; Bradshaw, J. S.; Cowan, D. O.; Counsell, R. C.; Vogt, V.; Dalton, J. C. *J. Am. Chem. Soc.* **1964**, *86*, 3197.

(6) Catalan, J.; Saltiel, J. *J. Phys. Chem. A.* **2001**, *105*, 6273.

(7) Wagner, P. J. *J. Am. Chem. Soc.* **1967**, *89*, 2820.

(8) Wagner, P. J.; Scheve, B. J. *J. Am. Chem. Soc.* **1977**, *99*, 2888.

(9) Balzani, V.; Bolletta, F.; Scandola, F. *J. Am. Chem. Soc.* **1980**, *102*, 2152.

(10) Orlandi, G.; Monti, S.; Barigelleti, F.; Balzani, V. *Chem. Phys.* **1980**, *52*, 313.

(11) Gorman, A. A.; Hamblett, I.; Irvine, M.; Raby, P.; Stauden, M. C.; Yates, S. *J. Am. Chem. Soc.* **1987**, *109*, 4404.

(12) Brennan, C. M.; Caldwell, R. A.; Elbert, J. E.; Unett, D. J. *J. Am. Chem. Soc.* **1994**, *116*, 3460.

(13) Ni, T.; Caldwell, R. A.; Melton, L. A. *J. Am. Chem. Soc.* **1989**, *111*, 457.

(14) Bylina, A. *Chem. Phys. Lett.* **1968**, 509.

(15) Sandros, K. *Acta Chem. Scand.* **1964**, *18*, 2355.

(16) Ramamurthy, V.; Liu, R. S. H. *J. Am. Chem. Soc.* **1976**, *98*, 2935.

(17) Allonas, X.; Lalevée, J.; Fouassier, J. P.; Tachi, H.; Shirai, M.; Tsunooka, M. *Chem. Lett.* **2000**, 1090.

(18) Lalevée, J.; Allonas, X.; Louërat, F.; Fouassier, J. P.; Tachi, H.; Izumitani, A.; Shirai, M.; Tsunooka, M. *Phys. Chem. Chem. Phys.* **2001**, *3*, 2721.

(19) Buchanan, G. W.; Dawson, B. A. *Can. J. Chem.* **1976**, *54*, 790.

(20) Irie, H.; Tanaka, S.; Zhang, Y.; Koyama, J.; Taga, T.; Machida, K. *Chem. Pharm. Bull.* **1988**, *36*, 3134.

(21) Buchanan, G. W.; Dawson, B. A. *Can. J. Chem.* **1978**, *56*, 2200.

(22) Buchanan, G. W.; Dawson, B. A. *Can. J. Chem.* **1977**, *55*, 1437.

(23) Stewart, J. P. *MOPAC*, version 6.0; Report QCPE 455.

(24) Frisch, M. J.; Trucks, G. W.; Schlegel, H. B.; Gill, P. M. W.; Johnson, B. G.; Robb, M. A.; Cheeseman, J. R.; Keith, T.; Petersson, G. A.; Montgomery, J. A.; Raghavachari, K.; Al-Laham, M. A.; Zakrzewski, V. G.; Ortiz, J. V.; Foresman, J. B.; Cioslowski, J.; Stefanov, B. B.; Nanayakkara, A.; Challacombe, M.; Peng, C. Y.; Ayala, P. Y.; Chen, W.; Wong, M. W.; Andres, J. L.; Replogle, E. S.; Gomperts, R.; Martin, R. L.; Fox, D. J.; Binkley, J. S.; Defrees, D. J.; Baker, J.; Stewart, J. P.; Head-Gordon, M.; Gonzalez, C.; Pople, J. A. *Gaussian 94*, revision E.3; Gaussian, Inc.: Pittsburgh, PA, 1995.

(25) Farmilo, A.; Wilkinson, F. *Chem. Phys. Lett.* **1975**, *34*, 575.

(26) Place, I.; Farran, A.; Deshayes, K.; Piotrowiak, P. *J. Am. Chem. Soc.* **1998**, *120*, 12626.

(27) Monti, S.; Gardini, E.; Bortolus, P.; Amouyal, E. *Chem. Phys. Lett.* **1981**, *77*, 115.

(28) Berry, R. J.; Douglas, P.; Garley, M. S.; Jolly, T.; Clarke, D.; Moglestue, H.; Walker, H.; Winscom, C. *J. Photochem. Photobiol. A: Chem.* **1999**, *120*, 29.

(29) Abu-Hasanayn, F.; Herkstroeter, W. *J. Phys. Chem. A.* **2001**, *105*, 1214.

(30) Marciniak, B.; Hug, G. L. *Coord. Chem. Rev.* **1997**, *159*, 55.

(31) Segawa, K.; Kikuchi, O.; Arai, T.; Tokumaru, K. *J. Mol. Struct. (THEOCHEM)* **1995**, *343*, 133.

(32) Brink, M.; Jonson, H.; Ottosson, C. *J. Phys. Chem. A.* **1998**, *102*, 6513.

(33) Davies, M. K.; Gorman, A. A.; Hamblett, I.; Unett, D. J. *J. Photochem. Photobiol. A: Chem.* **1995**, *88*, 5.